JOURNAL OF RHEOLOGY

Viscoelastic coalescence of thermotropic liquid crystalline polymers: The role of transient rheology

Eric Scribben, Aaron P. R. Eberle, and Donald G. Baird

Citation: Journal of Rheology (1978-present) **49**, 1159 (2005); doi: 10.1122/1.2039827
View online: http://dx.doi.org/10.1122/1.2039827
View Table of Contents: http://scitation.aip.org/content/sor/journal/jor2/49/6?ver=pdfcov
Published by the The Society of Rheology

Viscoelastic coalescence of thermotropic liquid crystalline polymers: The role of transient rheology

Eric Scribben, Aaron P. R. Eberle, and Donald G. Baird[a)]

Department of Chemical Engineering, Virginia Polytechnic Institute and State University, Blacksburg, Virginia 24061

(Received 13 August 2004; final revision received 7 July 2005)

Synopsis

The coalescence in air of two polymeric drops into a single drop (also referred to as sintering) was investigated for two thermotropic liquid crystalline polymers. Initial coalescence via elastic contact was ruled out based on the magnitude of the equilibrium compliance values and the process was, therefore, believed to be driven by surface tension and resisted by means of viscous flow. Remarkably the viscous coalescence model developed for Newtonian fluids (an extension of the Frenkel and Eshelby approach) agreed well under some conditions of temperature with coalescence data (i.e., observation of neck growth under a microscope). On the other hand, the extension of the Newtonian model to the viscoelastic case by incorporating the upper convected Maxwell model (UCM) assuming steady state stresses always underpredicted the rate of coalescence. The viscous neck growth model using the UCM constitutive equation was extended to the transient stress case in order to incorporate the slow growth of viscosity at the startup of flow. The unsteady state UCM approach represented a qualitative improvement over the Newtonian and steady state UCM formulations because it predicted accelerated coalescence, relative to the Newtonian model, by increasing the relaxation time. However, the model was unable to quantitatively predict the experimental coalescence rates, as it overpredicted the acceleration of coalescence. © *2005 The Society of Rheology.* [DOI: 10.1122/1.2039827]

I. INTRODUCTION

When two molten polymeric particles or drops are brought into contact, they coalesce into a single drop as shown schematically in Fig. 1 as a result of adhesive and surface tension forces. Three distinct steps of this coalescence process have been identified [Lin *et al.* (2001)]: (1) elastic adhesive contact; (2) zipping contact growth driven by adhesive intersurface forces and resisted by viscoelastic deformation; and (3) stretching contact growth driven by surface tension and resisted by viscous flow (i.e., classical viscous sintering). In phase 1 (for short times) when drops are brought into contact, they instantaneously deform to create a finite contact surface. The theory for phase 1 of the coalescence process is based on balancing the work of adhesion against the work of elastic deformation and is referred to as the "JKR" theory [Johnson *et al.* (1971)]. This theory was later extended to viscoelastic materials by Schapery (1975) and later by Hui *et al.* (1998) to give the following expression for the dimensionless contact radius or the neck growth:

[a)]Author to whom correspondence should be addressed; electronic mail: dbaird@vt.edu

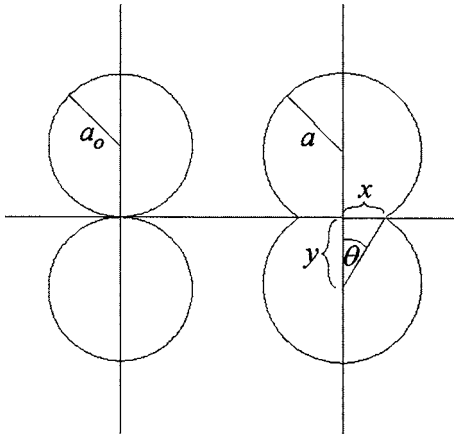

FIG. 1. Schematic of the geometric evolution of two coalescing spherical particles.

$$\frac{x}{a}=\left(\frac{9\pi C_0\Gamma}{a}\right)^{1/3}, \tag{1}$$

where C_0 is the equilibrium compliance (usually identified as J_e^0) and Γ is the surface tension for drops of identical diameter. For times $t \gg t_0$ [where t_0 is a characteristic time for which estimates are given in the paper by Lin and co-workers (2001)] but less than that for viscous flow, the dimensionless neck growth is given by

$$\frac{x}{a}=\left(\frac{63\pi^3}{16}\right)^{1/7}\left(\frac{\delta_c}{a}\right)^{2/7}\left(\frac{C_1\Gamma t}{a}\right)^{1/7}, \tag{2}$$

where δ_c is the range of the adhesive surface force and C_1 is a parameter in the power-law expression for the creep compliance ($C_1=1/\mu$ for a fluid). Finally, for long times, i.e., $t \gg t_v$, where t_v is the time for viscous flow [an expression for t_v is given in the paper by Lin *et al.* (2001)], Lin *et al.* (2001) proposed that Frenkel's theory (1945) for a Newtonian fluid could be used

$$\frac{x}{a}=\left(\frac{9C_1\Gamma t}{2a_0}\right)^{1/2}, \tag{3}$$

where a_0 is the initial radius of the drops and C_1 is $1/\mu$, where μ is the Newtonian viscosity.

For the polymeric materials studied by Mazur and Plazek (1994) which consisted of polytetrafluoroethylene and polymethylmathacrylate (PMMA) resins, the coalescence or sintering behavior was fit well by these models. These materials were more like soft solids rather than viscous fluids as the viscosity was of the order of 10^9 Pa and the coalescence times were of the order of 10^6 s. In particular, for times between 10^0 and 10^4 s coalescence was described by Eq. (2) ("zipping mode") whereas for $t > 10^4$ s coalescence was described by Eq. (3) (viscous flow).

For polymer melts various behavior has been observed depending on the size of the particles. Neck growth measurements on relatively large polystyrene and PMMA spheres ($R=250-300$ μm) have been reported to agree well with the viscous sintering model [Rosenweig and Narkis (1981)]. However, in the work of Kucynski and co-workers (1970) on smaller spheres ($R<120$ μm) of the same polymers significant contact growth

was observed at much earlier times than predicted by viscous sintering. This has prompted Mazur (1995) to propose that particles smaller than a certain critical size sinter completely by retarded elastic deformation and without any contribution from viscous flow.

It is remarkable that for several polymers and silicate glasses that the viscous sintering model as described in Eq. (3) predicted neck growth extremely well as Eq. (3) is really limited to the early stages of neck growth (i.e., small angles of θ in Fig. 1) and not for late stages. Furthermore, there are a number of assumptions in the development of Eq. (3) which could limit its utility as discussed next.

The model for the coalescence of two viscous drops as first proposed by Frenkel (1945) and Eshelby (1949) was derived from the mechanical energy balance by equating the work of surface tension to the work done by the rheological stresses, which is referred to as viscous dissipation for a purely viscous fluid [Bird *et al.* (1987)]. External stresses and gravitational effects were neglected and the flow kinematics were assumed to be biaxial stretching flow. The rheological stresses were assumed to be described in terms of the Newtonian constitutive equation. Despite its simplicity by assuming a constant viscosity and particle radius, the Frenkel model defines a relationship between material properties, drop size, and the neck growth rate for a viscous fluid that has agreed at least qualitatively with experimental data by illustrating that the rate of neck growth can be increased by either increasing surface tension or decreasing the viscosity. Actually the model has also demonstrated good quantitative agreement with measured values of the dimensionless neck radius, x/a, and the predicted exponent of $1/2$ on time for simple glassy materials and several polymers [Kuczynski *et al.* (1970); Bellehumeur *et al.* (1998)]. Furthermore, finite element simulations of coalescence of a Newtonian fluid agree well with the theory and even confirm that the flow is primarily biaxial extensional except in the neck region [Jagota *et al.* (1988); Martinez-Herrera and Derby (1995)].

Several improvements in the viscous sintering model have been proposed recently. Pokluda *et al.* (1997) improved the accuracy of the Newtonian model by deriving an expression for the change in particle radius, $a(t)$, based on conservation of volume. Bellehumeur *et al.* (1998) developed a viscoelastic coalescence model using the upper convected Maxwell (UCM) constitutive model in Frenkel's approach along with Pokluda's expression for particle radius. As a first approximation, they assumed that the stresses were at steady state at any instant during the coalescence process. Using arbitrarily selected increasing values of the relaxation time, they found that the steady state UCM coalescence model was in close agreement with their experimental data for several polymer melts suggesting that for viscoelastic fluids that elastic adhesive contact (step 1) and zipping contact growth (step 2) may not be significant at least for polymer melts with zero shear viscosity values of less than 10^5 Pa s.

The steady state UCM neck growth model predicted that the neck growth rate decreased as the relaxation time was increased. This predicted behavior supported the assertion that viscoelasticity was responsible for the slow coalescence of the polymers investigated by Bellehumeur *et al.* (1998), relative to the Newtonian model. However, the behavior predicted by the steady state UCM neck growth model is not generally applicable to all viscoelastic fluids because reported coalescence times for polytetrafluoroethylene and several acrylic resins were significantly shorter than what were predicted by the Newtonian model [Mazur (1995); Mazur and Plazek (1994)]. We note, however, that the viscosity of the materials used by Mazur and Plazek was five orders of magnitude higher than that of the polymers used by Bellehumeur. Furthermore, the relaxation times used in the steady state UCM neck growth model were not measured experimentally. Instead, they were arbitrarily increased to produce better agreement with the data, and

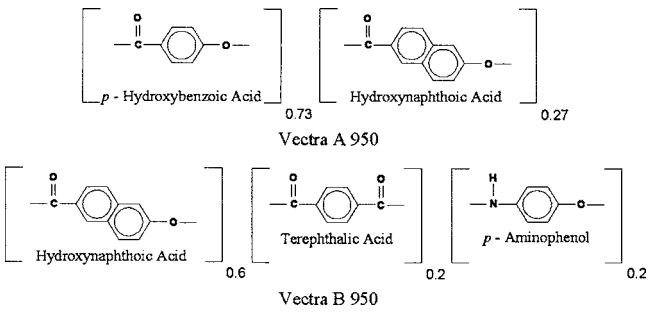

FIG. 2. Chemical structure and composition of Vectra A 950 and Vectra B 950.

these values were unrealistically large. However, by arbitrarily picking the relaxation times to fit the coalescence data, the model at least predicted the correct dependence of neck growth on time, suggesting that the sintering process was dominated by viscous flow for viscoelastic polymer melts.

In this paper, we are particularly interested in the coalescence behavior of two thermotropic liquid crystalline polymers (TLCPs). In initial work, the coalescence behavior of two commercial TLCPs was studied in an effort to identify the conditions which would lead to their successful sintering [Scribben and Baird (2002)]. It was observed that coalescence was possible at temperatures where the material exhibited a fairly well-defined zero shear viscosity and not the yield-like viscosity behavior observed in some liquid crystalline polymeric systems. The yield-like behavior has also been referred to as region I in the three-region viscosity description by Onogi and Asada (1980), where shear thinning at low shear rates followed by a rate independent plateau at moderate rates (region II) and another shear thinning region at high rates (region III). Furthermore, it was observed that the two TCLPs coalesced at the same rate at one temperature even though their low shear rate viscosities were significantly different. Because their viscosity is relative low and in the range of most polymer melts, it is believed that elastic adhesive contact (step 1) and zipping contact growth (step 2) may not be significant relative to viscous flow. For this reason the objective of this work is to determine if the coalescence behavior of two TLCPs can be quantitatively predicted by extending the neck growth model of Frenkel and Eshelby to include the transient viscosity behavior through the use of the UCM constitutive equation. To accomplish this objective, two TLCPs with markedly different rheological behavior are used. Predictions from the Newtonian, steady state UCM, and the transient UCM neck growth models are compared to experimental data to determine not only if the transient UCM model can improve the accuracy of the predictions but help explain the observed coalescence behavior.

II. EXPERIMENT

A. Materials

Two TLCPs which are believed to exhibit nematic order, Vectra A 950 and Vectra B 950, available from Ticona (Summit, NJ), were selected for this evaluation. Both materials are randomly copolymerized wholly aromatic copolyesters: Vectra A is composed of hydroxybenzoic acid and hydroxynaphthoic acid, and Vectra B is composed of hydroxynaphthoic acid, terephthalic acid, and aminophenol [Beekmans *et al.* (1997); Wilson (1991)]. The chemical structure and mole fraction of each monomer are shown in Fig. 2. The melt temperature, as determined by the peak value from differential scanning calo-

rimetry (DSC), is 282 °C for Vectra A 950 and 279 °C for Vectra B 950 [Wilson (1991)]. When the melt is cooled quiescently, the crystallization temperature is 236 °C for Vectra A 950 and 226 °C for Vectra B 950, as defined by the beginning of the exothermic crystallization peak measured by DSC. However, it has been reported that Vectra A 950 may crystallize in shear flow at higher temperatures, up to approximately 300 °C [Beekmans *et al.* (1997)]. The glass transition temperatures, as measured by the peak value from dynamic mechanical thermal analysis, are 113 and 147 °C, for Vectra A 950 and Vectra B 950, respectively [Ticona (2002)]. The nematic to isotropic transition temperature is unknown because degradation occurs at temperatures below the transition. The weight average molecular weight and polydispersity index are not known but are thought to be around 30 000 and 2, respectively, for both materials [Wilson (1991)]. The materials were dried, in accordance to manufacturer specifications, in a vacuum oven at 150 °C for between 12 and 24 h, before the measurement of surface tension, rheological characterization, or neck growth experiments.

B. Differential scanning calorimetry

DSC was used to identify a potential minimum temperature for the neck growth experiments by measuring the end of the melt transition. The thermal analysis was performed with a heating rate of 10 °C/min with a Seiko Instruments SSC/5200 series auto cooling DSC-220C. The sample was exposed to both a heating and a cooling cycle before the recorded measurement to ensure the material had been properly dried and to impose a known thermal history. Two temperatures, 320 and 330 °C, were selected for the neck growth experiments because they were at least 10°–15° greater than the end of the melt transitions. However, it should be noted that DSC cannot be used solely to determine conditions for TLCP coalescence because thermal analysis provides no means of determining if region I viscosity behavior is present.

C. Surface tension measurement

The surface tension of each of the materials was determined by fitting the Bashforth and Adams equation to the sessile drop profile of the molten polymer in an inert atmosphere at 320 and 330 °C [Padday (1969)]. This method was selected because it presents a noninvasive means of measuring the surface tension of the TLCP as a melt with the identical geometry, thermal history, and deformation history of the particles used in the neck growth experiments. A single 500 μm diameter sphere was placed on a glass slide in the hot stage, where it was melted into a sessile drop. A description of the procedure used to generate the spherical particles is provided in detail elsewhere [Scribben (2004)] but is based on a blending process carried out in a single screw extruder and then a separation technique to remove the spherical particles from the matrix polymer. The sample was quenched and the glass slide was rotated to allow a profile view of the drop from above. The sample was reheated to the test temperature and a digital image of the profile was recorded by an optical microscope equipped with a mini DV camcorder. The Bashforth and Adams equation was fit to data points representing the profile shape that were extracted from the digital image of the profile with Scion Image, an image analysis software available from Scion Corporation. The accuracy of this technique (0.1%) demands that the particle radii must be small so that gravitational forces cannot influence the shape of the profile. The absence of gravitational forces was verified by calculating the Bond number $\mathrm{Bo}=\rho r^2 g/\Gamma$ (0.027 for Vectra A 950 and 0.030 for Vectra B 950) and was supported by the observation that the profile shape did not change upon rotating the glass slide.

TABLE I. Coalescence model parameters and calculated values of the Deborah number.

	Temperature (°C)	Relaxation time λ (s)	Viscosity $\eta(0.01\ s^{-1})$ (Pa s)	Surface tension Γ ±0.002 (J/m^2)	Particle radius a_0 ±1 (μm)	De $(\lambda\Gamma/\eta_0 a_0)$	J_e^0 Pa^{-1}
Vectra A 950	320	50.8	2301	0.031	250	2.7	0.031
	330	49.3	2809	0.031	250	2.2	0.031
Vectra B 950	320	3.04	257	0.029	250	1.4	1.54
	330	2.97	384	0.029	250	0.9	3.86

D. Rheological characterization

Rheological characterization in steady and transient shear flow was performed with a Rheometrics mechanical spectrometer model 800 (RMS-800). The instrument test geometry was a 25 mm diameter cone and plate with a 0.1 rad cone angle. The magnitude of the complex viscosity, $|\eta^*|$, versus angular frequency, ω, and shear viscosity, η, versus shear rate, $\dot{\gamma}$, data were measured in the presence of an inert nitrogen atmosphere to prevent thermo-oxidative degradation. Test specimens were prepared by compression molding preforms from pellets at 320 °C under nominal pressure and allowing them to quiescently cool without applied pressure. This method produces homogeneous samples with minimal residual stress that geometrically match the cone and plate test fixtures. Reported rheological results represent the average of at least three runs using different samples for each run. Small amplitude dynamic oscillatory shear measurements were performed for angular frequencies between 0.01 and 100 rad/s at 10% strain at both 320 and 330 °C. The steady shear viscosity was measured at low shear rates, below 0.1 s^{-1}, by recording the steady state value of a stress growth upon inception of steady shear flow experiment. The stress growth experiments were performed because of the lengthy times required to obtain data at low angular frequencies from dynamic oscillatory measurements. Transient viscosity values at shear rates less than or equal to 0.01 s^{-1} were thought to be the most pertinent to the coalescence process and were used to obtain parameters for the UCM constitutive model by minimizing the sum of the squared difference between the predicted and experimental transient viscosity values at 0.01 s^{-1}. Model fitting was performed at 0.5 s intervals from inception of flow until steady state was achieved.

Creep measurements were carried out on a RSR-8600 (Rheometrics, Inc.) to obtain the equilibrium creep compliance, J_e^0. These measurements were performed at shear stress levels which were in a range approaching zero shear-like viscosity behavior at 320 and 330 °C. For Vectra B a shear stress of 0.3 Pa was used while for Vectra A950 2 Pa was used. A constant shear stress was applied to all materials until steady state creep was reached. J_e^0 was obtained by extrapolating $J(t)$ at steady state conditions to zero time [Macosko (1994)]. The repeatability of these measurements based on five repeat runs was found to be ±20%. The values of J_e^0 are listed in Table I for each resin.

E. Neck growth experiments

The kinetics of coalescence was determined by means of neck growth measurements for the TLCP particles at two temperatures, 320 and 330 °C. Two spherical particles with a diameter of 500 μm, identical to those used in the surface tension measurements, were placed in contact inside a Linkam THM 600 hot stage set at one of two operating temperatures, as identified by the DSC and shear viscosity measurements. The tests were

performed in an inert, nitrogen atmosphere to assist in eliminating thermo-oxidative degradation during the experiment. The heating rate for the neck growth experiments was 90 °C/min and the test temperature was maintained at the set point to within 0.1 °C, which provided nearly isothermal conditions. The neck growth process was observed in the hot stage with a Zeiss Axioskop equipped with a color charge coupled device camera. The video feed was recorded to high resolution digital video. The neck growth between the two particles was identical to that shown schematically in Fig. 1. Still images from the digital video were extracted at prescribed intervals, and the neck and particle radii were measured using Scion Image, a digital image analysis software available from Scion Corporation. Each neck growth experiment was conducted three times to ensure reproducibility, and the reported neck radius versus time data is the average of the three runs.

III. THEORY FOR VISCOLEASTIC COALESCENCE

The starting point for viscoelastic coalescence is based on the approach used by Frenkel to develop a viscous coalescence model which began with performing a mechanical energy balance that equated the work of surface tension to the work done by the rheological stresses, which is referred to as viscous dissipation for a purely viscous fluid [Bird *et al.* (1987)]

$$-\Gamma\frac{dS}{dt}=\int\int\int \boldsymbol{\sigma}:\mathbf{D}dV, \tag{4}$$

where Γ is surface tension, S and V are the surface area and volume of both spheres, respectively, $\boldsymbol{\sigma}$ is the deviatoric stress tensor, and $\mathbf{D}$ is the rate of strain tensor:

$$\mathbf{D}=\frac{1}{2}(\boldsymbol{\nabla}\mathbf{v}+\boldsymbol{\nabla}\mathbf{v}^{T}), \tag{5}$$

where the components of the velocity gradient tensor are given by,

$$\boldsymbol{\nabla}\mathbf{v}=\begin{bmatrix}\dot{\varepsilon} & 0 & 0\\ 0 & -2\dot{\varepsilon} & 0\\ 0 & 0 & \dot{\varepsilon}\end{bmatrix} \tag{6}$$

and $\dot{\varepsilon}$ is the extension rate. Frenkel's approach has since been reformulated to account for change in the drop radius during the process to produce a homogeneous, first-order differential equation for determining the angle θ, as outlined by Pokluda *et al.* (1997)

$$\frac{d\theta}{dt}=\frac{\Gamma}{\eta a_0}\frac{2^{-5/3}\cos(\theta)\sin(\theta)}{K_1^2[2-\cos(\theta)]^{5/3}[1+\cos(\theta)]^{4/3}}, \tag{7}$$

where K_1 is defined (overall all angles during the neck growth process) by [Scribben (2004)]

$$K_1=\frac{\tan\theta}{2}-\frac{\sin\theta}{6}\left[\frac{2(2-\cos\theta)+(1+\cos\theta)}{(1+\cos\theta)(2-\cos\theta)}\right]. \tag{8}$$

Bellehumeur *et al.* (1998) evaluated Eq. (7) for η replaced by μ (the Newtonian neck growth model) for several polyethylenes and propylene/ethylene copolymers. It was found that the model overpredicted the neck growth rates of the selected polymers [Bellehumeur *et al.* (1998)]. They attributed the model's inaccuracy to the viscoelastic rheological behavior of the polymers and proposed an extension of the Newtonian neck growth model that incorporated viscoelastic effects by using the UCM constitutive equa-

tion to describe the extra stress tensor. They assumed the flow field was homogeneous and the stresses, at any instant, were at steady state, although the stresses may change because the extension rate is not constant throughout the process. The reader is referred to the original paper for details on the complete derivation of the steady state UCM neck growth model, which is given by [Bellehumeur *et al.* (1998)]

$$8\left(\lambda K_1 \frac{d\theta}{dt}\right)^2 + \left(-2\lambda K_1 + \frac{a_0 \eta}{\Gamma}\frac{K_1^2}{K_2}\right)\frac{d\theta}{dt} - 1 = 0, \tag{9}$$

where λ is the characteristic relaxation time and,

$$K_2 = \frac{2^{-5/3}\cos\theta \sin\theta}{(1+\cos\theta)^{4/3}(2-\cos\theta)^{5/3}}. \tag{10}$$

By arbitrarily increasing values of λ they could accurately predict the observed coalescence for the polymer melts, but the value was unrealistically high (e.g., 400 s). This could be due to the fact that at a critical biaxial extension rate, $\dot{\varepsilon}_c = 1/2\lambda$, the biaxial extensional viscosity approaches infinity which would retard coalescence.

Here we extend the approach discussed above to the UCM neck growth model without the steady state assumption, which is described by Eqs. (11)–(13) (hereafter it is referred to as the transient UCM neck growth model because of the use of transient rheological stresses). Equation (7) is rewritten in terms of the transient biaxial extensional viscosity to give

$$\frac{d\theta}{dt}\frac{2^{2/3}a_0\eta_b K_1^2}{3\Gamma}\frac{(1+\cos\theta)^{4/3}(2-\cos\theta)^{5/3}}{\cos\theta\sin\theta} - 1 = 0, \tag{11}$$

where η_b is given by

$$\eta_b = e^{-[(1/\lambda)2\dot{\varepsilon}]t}\left[\frac{2\eta}{(1-2\lambda\dot{\varepsilon})}e^{[(1/\lambda)2\dot{\varepsilon}]t} + \frac{C_1}{\dot{\varepsilon}}\right] + e^{-[(1/\lambda)+4\dot{\varepsilon}]t}\left[\frac{4\eta}{(1+4\lambda\dot{\varepsilon})}e^{[(1/\lambda)+4\dot{\varepsilon}]} + \frac{C_2}{\dot{\varepsilon}}\right], \tag{12}$$

where C_1 and C_2 are determined from

$$C_1 = \left[\sigma_{11}(t_n) - \frac{2\eta\dot{\varepsilon}}{(1-2\lambda\dot{\varepsilon})}\right] \quad C_2 = \left[\sigma_{22}(t_n) + \frac{4\eta\dot{\varepsilon}}{(1+4\lambda\dot{\varepsilon})}\right] \tag{13}$$

at some time t_n prior to time, t, where the extension rate is defined by

$$\dot{\varepsilon} = -\frac{1}{2}\frac{\partial v_y}{\partial y} = K_1\frac{d\theta}{dt}. \tag{14}$$

The transient model is solved using the following procedure. At the beginning of a time step the value of the coalescence angle $\theta_n = \theta(t_n)$, is known, either from the initial condition (which is discussed later) or the previous time step. The extension rate is assumed to be constant over a time step and, hence, the corresponding rate of the coalescence angle at time t_n, $(d\theta/dt)_n$, is obtained by determining the root of Eq. (11) using Müller's method. At the end of a time step, the stresses and extension rate are updated and used to determine the constants C_1 and C_2 for the next step. Finally, the new coalescence angle, θ_{n+1}, is determined using a forward difference formula. Convergence was achieved when there was less than 0.01% difference in each predicted value of dimensionless neck growth between successive reductions of the time step.

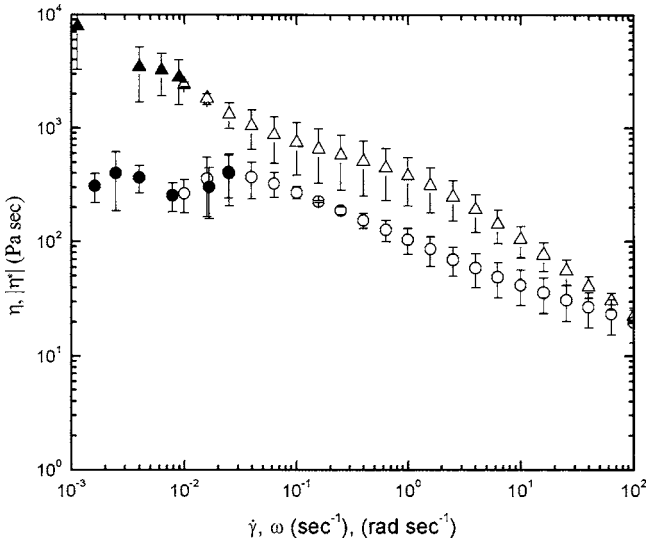

FIG. 3. Steady and complex shear viscosity master curves for Vectra A 950 (△) and Vectra B 950 (○) at 320 °C. The open symbols represent small amplitude oscillatory shear measurements and the filled symbols represent steady shear values.

IV. RESULTS AND DISCUSSION

A. Rheological characterization

The results from steady shear and small amplitude dynamic oscillatory measurements are shown in Figs. 3 and 4. Despite the inherent difficulty in performing rheological measurements at low shear rates and frequencies, the magnitudes of the steady shear and

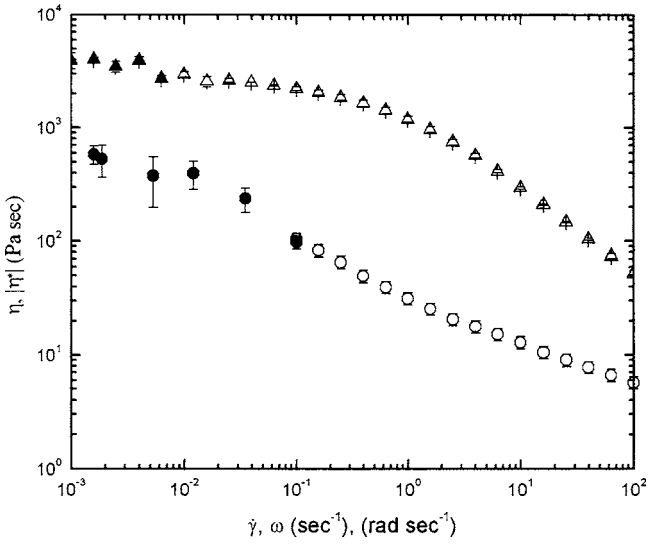

FIG. 4. Steady and complex shear viscosity master curves for Vectra A 950 (△) and Vectra B 950 (○) at 330 °C. The open symbols represent small amplitude oscillatory shear measurements and the filled symbols represent steady shear values.

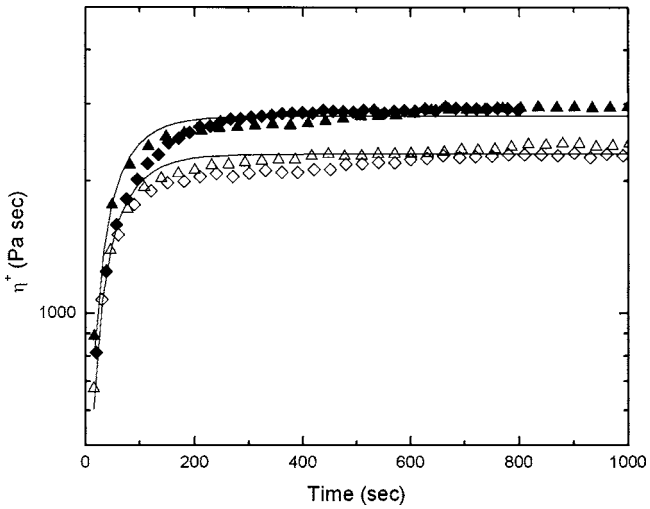

FIG. 5. The transient shear viscosity for Vectra A 950 measured at a shear rate of 1×10^{-2} s^{-1}: (△) at 320 °C and (▲) at 330 °C, repeated results: (◇) at 320 °C and (◆) at 330 °C. The lines represent the fits of the single mode upper convected Maxwell model to the data.

complex viscosities agree well. It was also found that Vectra A 950 at 320 °C did not exhibit a zero shear viscosity over the measured range of deformation rates tested. The measured steady shear viscosity at low deformation rates exhibited region I viscosity behavior. Vectra B 950 at 320 °C did not exhibit region I viscosity behavior for shear rates below 1×10^{-2} s^{-1}, and the magnitude of the viscosity was approximately an order of magnitude less than that measured for Vectra A 950. At 330 °C, neither of the materials exhibited region I viscosity behavior at shear rates below approximately 1×10^{-2} s^{-1}, which is a significant change for Vectra A 950 relative to the values measured at 320 °C. Also, at 330 °C the magnitude of the shear viscosity of Vectra A 950 at low rates was approximately an order of magnitude greater than the shear viscosity of Vectra B 950. Furthermore, the viscosity at low shear rates of Vectra B 950 tended to increase slightly relative to that at 320 °C which may be do to the decrease of liquid crystalline order as the temperature is increased, which is common for polymeric fluids with liquid crystalline order [Wissbrun (1981)]. Certainly at higher shear rates the viscosity is observed to decrease with increasing temperature.

Representative transient viscosity data are shown for Vectra A 950 in Fig. 5 for two test temperatures. The transient shear viscosity curves for Vectra A 950 at 330 °C and Vectra B 950 at both test temperatures were highly repeatable. Furthermore, the fit of the single mode UCM model is shown in Fig. 5. The single mode UCM model, despite not being designed to for modeling complex fluids such as TLCPs, represents the transient shear viscosity data well at the test conditions as illustrated by this representative example for Vectra A 950. The fit of the UCM model was concentrated at times up to about 50 s which covered the time of the coalescence experiments. It is also interesting to note that the steady state stress values at 330 °C are higher than those at 320 °C which is reflective of the complex structure present in these materials. However, under the conditions used the fluids were believed to be globally anisotropic initially as the domains were randomly oriented. A summary of the coalescence model parameters and calculated Deborah numbers, as defined for coalescence, is provided in Table I.

We realize that the UCM may not be appropriate for TLCPs, even though the stress

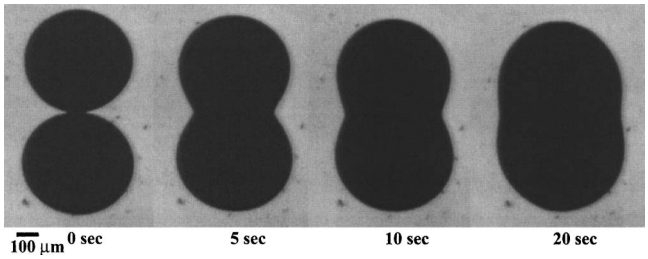

FIG. 6. Optical micrographs from the neck growth experiments of Vectra B 950 at 320 °C.

growth behavior is fit well by the single mode UCM model and the stress growth data look similar to that of common isotropic polymer melts. There have been reports of oscillations of the shear stresses during start up of steady shear flow [Ternet *et al.* (2001)]. There have also been reports of interesting behavior in the normal stress differences, such as negative values at steady state or local minima before reaching steady state [Wilson (1991)]. Despite the complex behavior exhibited by some TLCPs that suggests a complex constitutive equation may need to be considered, it is possible that the rheological behavior of TLCPs during coalescence can be sufficiently described by a more conventional viscoelastic constitutive model. The dimension of the liquid crystalline domains for the materials evaluated in this study is on the order of 1 μm, while the particle diameter is approximately 500 μm [Gotsis and Odriozola (2000)]. The particles were prepared in such a manner that the liquid crystalline domains were not preferentially oriented {a description of the process is provided elsewhere, but is essentially based on drop deformation and breakup in shear flow [Scribben (2004)]}. Therefore, without preferential orientation of the domains, a random distribution of orientation exists and the particle is effectively isotropic on the 500 μm scale. A possible influence of negative values of the primary normal stress differences should not be a factor because the flow kinematics for neck growth are primarily biaxial extension. In addition, the transient biaxial extensional viscosity can be approximated by the transient shear viscosity, using the relationship, $\eta_b^+ = 6\eta_0^+$, which was verified for these materials for deformation rates ($\dot{\varepsilon}, \dot{\gamma}$) up to 0.1 s^{-1} [Done (1987)].

B. Neck growth behavior

A representative example of the micrographs recorded during neck growth is shown in Fig. 6 for Vectra B 950, where there is initially a finite contact radius of x/a of about 0.1–0.2 and the neck radius increases with time until the two drops converge. In the example, the two particles nearly reached a dimensionless neck radius of 1 within 30 s. Although the test was stopped a few seconds later because the magnitude of the change in the dimensionless neck radius became comparable to the magnitude of the error in the measurement, the two particles did appear to continue to coalesce towards a single, nearly spherical drop.

Before discussing neck growth, the initial contact radius must be discussed as this value is important to the initial conditions for the calculations. Typically the value of x/a was observed to be about 0.1–0.2. Values of the initial contact radius based on using Eq. (1) and the parameters provided in Table I ranged from 4 to 20 which are highly unreasonable considering the maximum value of x/a is 1.0. Hence, the initial value cannot be due to elastic contact. It is possible that some viscous growth occurs during the time of heating from the melting point to the coalescence temperature.

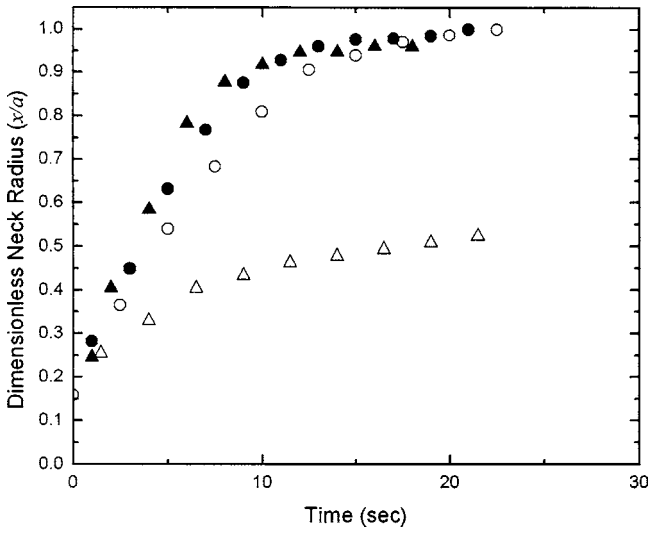

FIG. 7. TLCP neck growth data, where (△) represents Vectra A 950 and (○) represents Vectra B 950. Open symbols are used for the data at 320 °C and filled symbols represent the data at 330 °C.

Neck growth data is shown in Fig. 7 for Vectra A 950 and Vectra B 950 at both temperatures. The neck growth rate for Vectra A 950 at 320 °C was slower than that for Vectra A 950 at 330 °C and Vectra B 950 at both temperatures. It was also observed that Vectra A 950 failed to completely coalesce at 320 °C, which may be explained by the presence of the region I shear viscosity behavior at that temperature. The yield-like behavior that occurs in region I may be explained by the presence of residual crystallites. Lin and Winter (1988, 1991) and Wilson (1991) showed that residual crystallites were present in the melt at 320 °C, but were completely melted by 330 °C for Vectra A 950. If residual crystallites were present in Vectra A 950 at 320 °C, they may have acted as physical crosslinks, effectively increasing the viscosity and, hence, slowing neck growth.

V. COMPARISON OF COALESCENCE DATA TO CALCULATED VALUES OF NECK GROWTH

We next turn our attention to whether the Newtonian solution [Eq. (7)] or the solution using the steady UCM model [Eq. (9)] could account for the observed coalescence behavior. To solve these equations we used the initial value of 0.15 which was typically observed experimentally. Bellehumuer and co-workers (1998) used the small angle solution [Eq. (3)] at times of 0.0001 s to estimate the initial value of x/a, but without justification for this choice. In Fig. 8 the coalescence behavior at 320 °C is compared against the model predictions. For Vectra B using the parameters given in Table I it is observed that the Newtonian model predicts that coalescence will occur in about 10 s whereas it is observed to occur in about 15 s. Hence, the Newtonian model predicts a faster coalescence than is observed, but the shape of the curve is nearly correct (i.e., the appropriate time dependence for viscous flow). The UCM model under steady state conditions significantly under predicts the coalescence rate of Vectra B. For Vectra A 950 at 320 °C (also Fig. 8) the agreement between the predictions of the Newtonian model and data are remarkably good while the UCM model significantly under predicts the coalescence rate. At 330 °C as shown in Fig. 9 the coalescence rate is the same for both Vectra A and Vectra B even though they have significantly different low shear rate

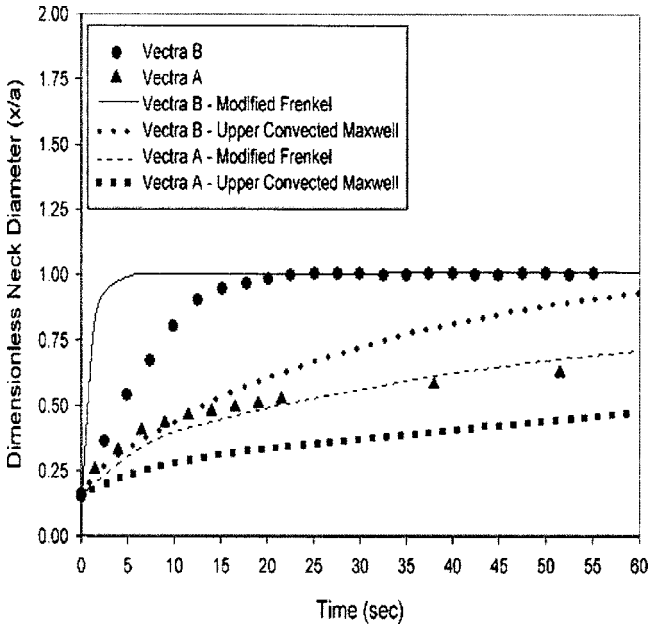

FIG. 8. Comparison of neck growth data with predictions of the Newtonian and steady state UCM model for Vectra A 950 and Vectra B at 320 °C.

viscosity values. The data agree well with the predictions of the Newtonian model for Vectra B using the data given in Table I. The agreement between data and the Newtonian model for Vectra A at 330 °C is poor as the Newtonian model significantly under predicts the coalescence rate. Again the UCM model predictions significantly under predict the coalescence rates for both materials.

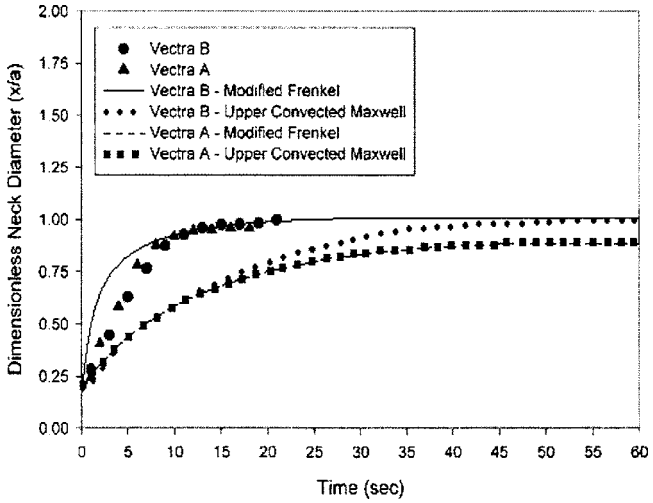

FIG. 9. Comparison of neck growth data with predictions of the Newtonian and steady state UCM model for Vectra A950 and Vectra B at 330 °C.

The Newtonian model in general does remarkably well at predicting the neck growth rate in some cases. In particular, it does well for Vectra A at 320 °C and Vectra B at 330 °C. On the other hand, it significantly under predicts the neck growth rate for Vectra A at 330 °C. In this work, the surface tension of each TLCP is independent of temperature and is approximately equal for both materials. According to the Newtonian model predictions, the driving force for coalescence is equivalent in all cases and the differences in the measured neck growth rates may be attributed to differences in the shear viscosity. As the shear viscosity is increased, the Newtonian model predicts a decrease in the neck growth rate. In this work, the magnitude of the shear viscosity for Vectra B 950 is slightly greater at 330 °C than at 320 °C, but, in contrast to what is suggested by the Newtonian model, neck growth is faster at 330 °C. In addition, as shown in Fig. 7, Vectra A 950 at 330 °C coalesces slightly faster than Vectra B 950 at either temperature, despite the steady shear viscosity of Vectra A 950 being approximately an order of magnitude greater than the steady shear viscosity of Vectra B 950. Therefore, the Newtonian model fails to predict the quantitative behavior of the neck growth rates for the TLCPs used in this work under all conditions, but the predictions are at least qualitatively correct in terms of curve shape and time dependence. This is remarkable considering the potential complex rheology of these materials.

The steady state UCM neck growth model is also incapable of explaining the qualitative behavior of the neck growth data and, in fact, exhibited worse agreement with the data than the Newtonian case. The steady state assumption effectively eliminates the time dependence of the biaxial extensional viscosity. Therefore, the Newtonian and the steady state UCM neck growth models predict the same values of biaxial extensional viscosity for small values of the relaxation time and the biaxial extension rate. Under these conditions, the steady state UCM neck growth model predicts nearly the same neck growth rate as the Newtonian neck growth model, which cannot explain the qualitative behavior of the experimental data. As the biaxial extension rate is increased, the biaxial extensional viscosity passes through a slight minimum before beginning its increase towards infinity. An increase in the viscosity further reduces the neck growth rate relative to the Newtonian model. This effect does not explain the qualitative behavior of the neck growth data in Fig. 7. As reported in Table I, Vectra A 950 at 330 °C has a longer relaxation time than the values for Vectra B at either temperature. Therefore, the steady state UCM neck growth model predicts that Vectra A 950 coalesces more slowly than Vectra B 950 at either temperature, which is in disagreement with the experimental data.

A. Transient UCM neck growth model predictions

As observed in Fig. 5, at a shear rate of 0.01 s^{-1} it takes the viscosity of Vectra A about 200 s to reach steady state at both 320 and 330 °C. Considering coalescence occurred in most cases in less than 20 s, this suggests that the viscosity may never reach steady state and, hence, the effective viscosity is considerably less. Predictions based on the transient UCM, Newtonian, and UCM steady state neck growth models are shown for Vectra A 950 at 330 °C in Fig. 10. In essence, Eqs. (11)–(14) were solved numerically as discussed earlier using an experimentally observed initial value of $x/a=0.15$. Similar results were observed for Vectra A 950 and Vectra B at 320 °C (not shown here). As shown in the figure, the Newtonian neck growth model predictions began to deviate from the experimental data within the first few seconds and, afterwards, under predicted the neck growth rates. The steady state UCM neck growth model predicted slower coalescence than was predicted by the Newtonian model and, in doing so, was less accurate than the Newtonian model. The transient UCM neck growth model predicts greater neck growth

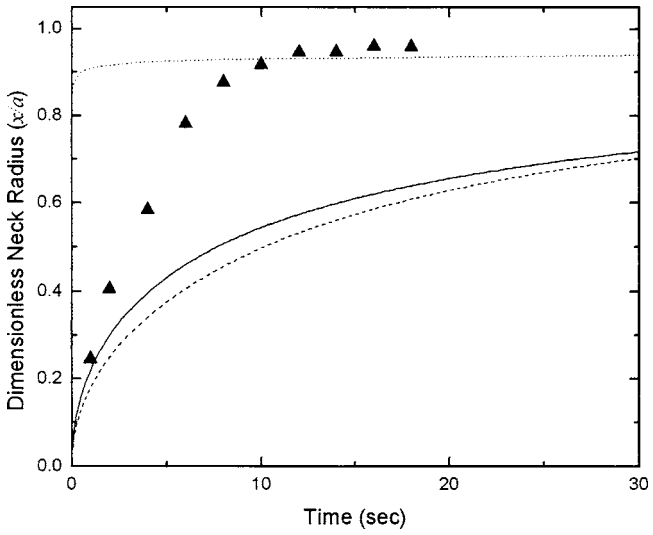

FIG. 10. Vectra A 950 neck growth data at 330 °C and predictions from the Newtonian, steady state UCM, and transient UCM neck growth models. The symbols represent the experimental data (▲) and the lines represent the neck growth model predictions: Newtonian (solid line), steady state UCM (dashed line), and the transient UCM (dotted line).

rates than the Newtonian model, which is in qualitative agreement with the experimental data. Unfortunately, the model grossly over predicts the neck growth rate, which is nearly instantaneous. Furthermore, the transient model gives almost identical results for both TLCPs at the two temperatures (data not shown). Also, the transient UCM neck growth model is unable to correctly predict the order of coalescence times for Vectra A 950 at 330 °C and Vectra B at 320 and 330 °C. The experimental coalescence times were $t_{\mathrm{VA330\,^\circ C}} < t_{\mathrm{VB330\,^\circ C}} < t_{\mathrm{VB320\,^\circ C}}$, as was shown in Fig. 7 and the model predicted $t_{\mathrm{VA330\,^\circ C}} < t_{\mathrm{VB320\,^\circ C}} < t_{\mathrm{VB330\,^\circ C}}$. Although the predicted results are not shown, the predicted order of coalescence times is consistent with the calculated Deborah number (see Table I), with the samples exhibiting larger Deborah numbers coalescing faster. It may be that multiple-relaxation times should be used as the shorter values in the spectrum will retard the coalescence of the drops. This along with a possibly more appropriate constitutive equation will be considered in future work.

VI. CONCLUSIONS

The coalescence of two TLCPs was studied by comparing experimentally measured values of the dimensionless neck radius with predicted values from the Newtonian, steady state, and the transient UCM neck growth models. Several significant conclusions can be drawn from this work. The first is that the behavior of the shear viscosity at low shear rates can be used to identify the temperature at which successful coalescence will occur. It was shown that the measured rheological behavior, specifically the transient viscosity in the limit of low shear rates, can be accurately represented by the UCM constitutive model. Finally, it was shown that the transient UCM neck growth model predicted faster neck growth than the Newtonian model, which was in qualitative agreement with the experimental data, but much faster. In spite of the potential for complex rheological behavior of the two TLCPs, coalescence seemed to be dominated by viscous flow rather than elastic contact.

ACKNOWLEDGMENTS

This work was financially supported by a phase II SBIR grant from NASA, Grant No. NAS-2S-4018-285, managed by Luna Innovations.

References

Beekmans, F., A. D. Gotsis, and B. Norder, "Influence of the flow history on stress growth and structure changes in the thermotropic liquid crystalline polymer Vectra B950," Rheol. Acta **36**, 82–95 (1997).

Bellehumeur, C. T., M. Kontopoulou, and J. Vlachopoulos, "The role of viscoelasticity in polymer sintering," Rheol. Acta **37**, 270–278 (1998).

Bird, R. B., R. C. Armstrong, and O. Hassager, *Dynamics of Polymeric Liquids, Volume 1 Fluid Mechanics* (Wiley, New York, 1987).

Done, D. D., "Studies on the rheology and morphology of thermotropic liquid crystalline polymers," Ph.D. dissertation, Virginia Polytechnic Institute and State University, Blacksburg, VA, 1987.

Eshelby, J. D., "Discussion" in Paper by A. J. Shaler, "Seminar on the kinetics of sintering," Trans. AIME **185**, 806–807 (1949).

Frenkel, J., "Viscous flow of crystalline bodies under the action of surface tension," J. Phys. (Moscow) **9**, 385–391 (1945).

Gotsis, A. D., and M. A. Odriozola, "Extensional viscosity of a thermotropic liquid crystalline polymer," J. Rheol. **44**, 1205–1223 (2000).

Hui, C. Y., J. M. Baney, and E. J. Kramer, "Contact mechanics and adhesion of viscoelastic spheres," Langmuir **14**, 6570–6578 (1998).

Jagota, A., and P. R. Dawson, "Micromechanical modeling of powder compacts. I. Unit problems for sintering and traction induced deformation," Acta Metall. **36**, 2551–2561 (1988).

Johnson, K. L., K. Kendall, and A. D. Roberts, "Surface energy and the contact of elastic solids," Proc. R. Soc. London, Ser. A **324**, 301–313 (1971).

Kuczynski, G. C., B. Neuville, and A. D. Roberts, "Sintering of poly(methyl methacrylate," J. Appl. Polym. Sci. **14**, 2069–2077 (1970).

Lin, Y. G., and H. H. Winter, "Structural relaxation behavior of a thermotropic liquid crystal aromatic copolyester in the super-cooled liquid state," Macromolecules **21**, 2439–2452 (1988).

Lin, Y. G., and H. H. Winter, "Formation of high melting crystal in a thermotropic aromatic copolyester," Macromolecules **24**, 2877–2892 (1991).

Lin, Y. Y., C. Y. Hui, and A. Jagota, "The role of viscoelastic adhesive contact in the sintering of polymeric particles," J. Colloid Interface Sci. **237**, 267–282 (2001).

Macosko, C. W., *Rheology Principles, Measurements, and Applications* (VCH, New York, 1994).

Martinez-Herrera, J. I., and J. J. Derby, "Viscous sintering of spherical particles via finite element analysis," J. Am. Chem. Soc. **78**, 645–665 (1995).

Mazur, S., "Coalescence of polymer particles," in *Polymer Powder Technology*, edited by M. Narkis and N. Rosenzweig (Wiley, New York, 1995), Chap. 8.

Mazur, S., and D. J. Plazek, "Viscoelastic effects in the coalescence of polymer particles," Prog. Org. Coat. **24**, 225–236 (1994).

Onogi, S., and T. Asada, "Rheology and rheo-optics of polymer liquid crystal," in *Rheology* edited by G. Astarita, G. Marrucci, and L. Nicholais (Plenum, New York, 1980), Vol. 1, pp. 127–147.

Padday, J. F., "Part II. The measurement of surface tension," in *Surface and Colloid Science*, edited by E. Matijević (Wiley Interscience, New York, 1969), Vol. 1.

Pokluda, O., C. T. Bellehumeur, and J. Vlachopoulos, "Modification of Frenkel's model for sintering," AIChE J. **43**, 3253–3256 (1997).

Rosenweig, N., and M. Narkis, "Sintering rheology of amorphous polymers," Polym. Eng. Sci. **21**, 1167–1170 (1981).

Schapery, R. A., "Theory of crack initiation and growth in viscoelastic media. I. Theoretical development," Int. J. Fract. **11**, 141–159 (1975).

Scribben, E., and D. G. Baird, "Sintering of thermotropic liquid crystalline polymers," Annu. Tech. Conf.-Soc. Plast. Eng. **60**, 1240–1244 (2002).

Scribben, E., "The selection of thermotropic liquid crystalline polymers for rotational molding," Ph.D. dissertation, Department of Chemical Engineering, Virginia Polytechnic Institute and State University, Blacksburg, VA, 2004.

Ternet, D. J., R. G. Larson, and L. G. Leal, "Transient director patterns upon start-up of nematic liquid crystals (an explanation for stress oscillation damping)," Rheol. Acta **40**, 307–316 (2001).

"Vectra® liquid crystal polymer (LCP)," Ticona, Summit, NJ, 2002.

Wilson, T. S., "The rheology and structure of thermotropic liquid crystalline polymers in extensional flow," Ph.D. dissertation, Department of Chemical Engineering, Virginia Polytechnic Institute and State University, Blacksburg, VA, 1991.

Wissbrun, K. F., "Rheology of rod-like polymers in the liquid crystalline state," J. Rheol. **25**, 619–662 (1981).